

The Influence of Physical Properties on the Durability and Compressive Strength of Fly Ash-Based Geopolymer Mortar under Tidal Acidic Exposure

Ratni Nurwidayati

Civil Engineering Program, Engineering Faculty, Lambung Mangkurat University, Indonesia | Agricultural Science, Lambung Mangkurat University, Indonesia
ratninurwidayat@ulm.ac.id

Akhmad Rizalli Saidy

Agricultural Science, Lambung Mangkurat University, Indonesia
asaidy@ulm.ac.id (corresponding author)

Nursiah Chairunnisa

Civil Engineering Program, Engineering Faculty, Lambung Mangkurat University, Indonesia
nursiah.chairunnisa@ulm.ac.id

Henry Wardhana

Civil Engineering Program, Engineering Faculty, Lambung Mangkurat University, Indonesia
henry.wardhana.ir@gmail.com

Mariamah

Civil Engineering Program, Engineering Faculty, Lambung Mangkurat University, Indonesia
mariamah5599@gmail.com

Received: 19 September 2025 | Revised: 17 October 2025 | Accepted: 24 October 2025

Licensed under a CC-BY 4.0 license | Copyright (c) by the authors | DOI: <https://doi.org/10.48084/etasr.14919>

ABSTRACT

The rising demand for cement and electricity has increased carbon emissions and produced large volumes of Fly Ash (FA) waste from coal power plants. Converting this waste into geopolymer mortar provides a sustainable alternative to conventional cement. This study used FA from the Asam-Asam Power Plant, activated with sodium silicate (Na_2SiO_3) and 8M sodium hydroxide (NaOH) in ratios of 1:1, 1.5:1, 2:1, and 2.5:1, with superplasticizer (SP) dosages from 0.1 to 0.3%. Mortar specimens were evaluated for water absorption, porosity, and sorptivity at 28 days and for compressive strength at 28 days and after up to three months of exposure to tidal acidic exposure. At 28 days, compressive strength reached 12.61 MPa. Secondary sorptivity was 0.0008–0.0023 $\text{mm s}^{-1/2}$ for the geopolymer mixes (minimum at SP3–R1.5) and 0.00071 $\text{mm s}^{-1/2}$ for the cement mortar; the initial 1–6 h segment satisfied the linearity criterion ($r \geq 0.98$) only for the cement mortar ($S_i=0.049 \text{ mm s}^{-1/2}$), indicating a divergence between mechanical strength and capillary transport. Geopolymers showed greater resistance to strength loss under tidal acidic exposure.

Keywords-geopolymer mortar; fly ash; porosity; sorptivity; tidal acidic exposure

I. INTRODUCTION

Indonesia's rapid infrastructure growth has sharply increased the demand for construction materials, especially concrete. Since cement forms 10–12% of concrete volume, rising demand has driven cement production upward [1].

Producing one tonne of cement emits about 0.7–1.1 tonnes of CO_2 [2], largely from limestone calcination, which contributes significantly to global warming. The cement industry alone accounts for 5–7% of global CO_2 emissions [3–5]. Reducing these emissions has become an urgent priority [5]. Proposed strategies include recycling cement, which can cut emissions

by up to 94% [6], and partial replacement of clinker with FA, limestone substitutes, or biomass fuels such as rice husks [7]. Energy use has also grown with infrastructure expansion. Electricity demand in Indonesia has continued to rise, increasing reliance on coal-fired power plants. Coal remains the dominant fuel for power plants, producing large amounts of FA and bottom ash (BA)—80–90% is FA [8].

Using FA in construction can reduce both carbon emissions and coal waste. Indonesian Government Regulation No. 22 of 2021 classifies coal combustion residues, including FA, as non-hazardous. High-volume fly ash (HVFA) concrete replaces 50–80% of cement, while geopolymers generally show higher strength, lower shrinkage, and better resistance to heat and chemicals [12–14]. However, challenges still exist regarding workability, viscosity, and long setting times [14].

FA from the Asam-Asam Power Plant has been studied for soil stabilization, emission control in peatlands, and as a material in bricks, paving blocks, and concrete [15–17]. Geopolymer strength largely depends on FA properties [18, 19]. The Asam-Asam Power Plant in South Kalimantan generates a significant amount of ash, similar to power plants in other regions [20]. While its blends with metakaolin and Bemban fiber [21] have been examined, fewer studies address key physical properties—porosity, density, absorption, and sorptivity—and their effect on performance. These factors are critical for understanding geopolymer mortar behavior.

Concrete also deteriorates rapidly in acidic environments. Portland cement is especially vulnerable as acids in peat water react with calcium compounds, leading to structural breakdown [22–24]. In tidal zones, cycles of wetting and drying accelerate

this process, reducing strength by nearly 20% in under two months [23]. Durability in such conditions is therefore essential. Geopolymer concrete performs better than Portland cement under acid attack [22, 25–28], but little is known about its behavior under repeated tidal exposure.

This study addresses that gap by examining how porosity, density, water absorption, and sorptivity affect the compressive strength and durability of Asam-Asam FA-based geopolymer mortar in tidal acidic exposure. Beyond performance, it highlights the potential of local industrial waste as a sustainable construction resource.

II. METHODOLOGY

A. Constituent Materials

FA was sourced from the Asam-Asam Power Plant in South Kalimantan, Indonesia. Table I reports the oxide composition measured by X-ray fluorescence (XRF). With a CaO content of 6.74% and a combined SiO₂, Al₂O₃, and Fe₂O₃ content of 86.29%, the values are consistent with those reported in [29]. Fly ash (FA) qualifies as Class F FA (ASTM C618) [30]. The specific gravity of FA was 2.83, bulk density 1.45 g/cm³, and fineness (retained on No.325, 45 μm) = 24%. The alkaline activator combined Na₂SiO₃ (SiO₂/Na₂O = 3.25, or 30.62% SiO₂ and 9.42% Na₂O) and 8M NaOH. A Type D Superplasticizer (SP) improved workability, dispersion, and compaction. Fine aggregate from a local quarry had a fineness modulus of 3.13, specific gravity of 2.70, water absorption of 1.63%, loose bulk density of 1.47 g/cm³, and compacted density of 1.60 g/cm³. The particle size distribution of fine aggregate in grading zone I. Tidal acidic exposure was simulated with a sulfuric acid solution with a pH of 3.

TABLE I. FA OXIDE COMPOSITION (WT%)

Oxide	SiO ₂	Al ₂ O ₃	Fe ₂ O ₃	CaO	MgO	Na ₂ O	K ₂ O	MnO ₂	TiO ₂	P ₂ O ₅	SO ₃
%	48.86	11.29	26.14	6.74	4.46	0.11	0.43	0.36	0.78	0.05	0.34

B. Mixture Design and Preparation

Unlike conventional concrete, the geopolymer mortars were proportioned by mass. Sodium silicate and 8M sodium hydroxide solutions were combined at Na₂SiO₃/NaOH mass ratios $R = 1.0, 1.5, 2.0, 2.5$. The precursor-to-activator proportion was FA: alkali = 60:40, i.e., $L/B = 0.67$ (liquid-to-binder). Fine aggregate to paste (FA + liquid) was 65:35, which corresponds to $S/B \approx 3.10$ (sand-to-binder). The SP was dosed at 0, 0.1, 0.2, or 0.3 wt.% of FA (coded SP0 to SP3).

For reproducibility, on a normalized basis of 1.00 kg FA, the total activator is $L = 0.67$ kg and is split as follows: $R = 1.0$: 0.334 kg Na₂SiO₃ + 0.333 kg 8M NaOH; $R = 1.5$: 0.400 kg + 0.267 kg; $R = 2.0$: 0.445 kg + 0.222 kg; $R = 2.5$: 0.476 kg + 0.191 kg. The corresponding fine-aggregate mass was 3.095 kg ($S/B \approx 3.10$). After casting, specimens were hardened at room temperature and then underwent two curing regimes: ambient curing (room-temperature storage) and moist curing (covered with a damp cloth for 28 days).

Mix IDs follow the format SP x -R y , where SP x represents the SP dosage (0, 0.1, 0.2, or 0.3 wt.% of FA, corresponding to

SP0–SP3), and R y denotes the Na₂SiO₃/NaOH mass ratio (1.0, 1.5, 2.0, or 2.5, corresponding to R1, R1.5, R2, and R2.5). For example, SP3-R1.5. The cement mortar used as a control is denoted as CM. When multiple mixes are presented, results are ordered by ascending R within each SP (SP0→SP3 if several SP levels appear), with CM listed last.

C. Experimental Procedures

1) Compressive Strength

Tests were performed at 14 and 28 days on 50 mm cubes, in accordance with ASTM C109 [31]. Before acid exposure, specimens were cured under two regimes: ambient curing (27±2°C, 70–80% RH) and moist curing (wrapped in damp cloth and rewetted daily). For the durability evaluation, only moist-cured cubes were exposed to H₂SO₄ adjusted to a pH of 3.0±0.1 under two scenarios: wet-dry cycling and continuous immersion. The term wet-dry cycles means that the cubes were immersed for 7 days, then air dried at ambient temperature for 7 days (one 14-day cycle). pH was checked every 24 hours and readjusted to 3.0±0.1. The solution was replaced weekly. The sequence was repeated for 3 months. Continuous immersion

means cubes remained submerged for 3 months with the same pH monitoring and weekly replacement. For both scenarios, the solution to the specimen volume ratio was 5:1. The compressive strength was then measured after 1, 2, and 3 months of exposure, and results are reported as mean \pm SD ($n = 3$) for each mix and condition. Figure 1(a) illustrates the specimens of geopolymer mortar, and Figure 1(b) shows the typical brittle failure under axial compression, showing shear wedges and lateral spalling.

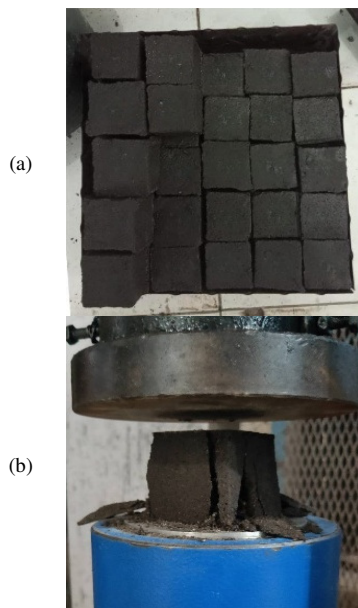


Fig. 1. (a) Geopolymer mortar before compressive testing; (b) typical brittle failure under axial compression.

2) Water Absorption, Density, and Porosity

These properties were tested only on SP3-R1, SP3-R1.5, SP3-R2, and SP3-R2.5. Tests followed ASTM C642-06 guidelines [32]. Three cylindrical specimens (100 \times 50 mm, volume 392.7 cm³) per mix were cured for 28 days. The specimens were oven-dried at 100–110°C for 24 hours, cooled, immersed in water for three days, boiled for five hours, and cooled for 14 hours before testing. Porosity was calculated as the difference between apparent density and bulk density, divided by the apparent density. SP3 mixtures, as the maximum SP dosage was expected to provide better workability and compaction, leading to more reliable evaluation of physical and transport properties.

3) Sorptivity

Sorptivity at 28 days was measured in accordance with ASTM C1585 [33] on SP3-R1, SP3-R1.5, SP3-R2, SP3-R2.5, and CM specimens. For each mix, three cylinders 100 \times 50 mm were oven-dried for 3 days, conditioned in sealed containers for 15 days, sealed on all faces except the exposed face, and tested in shallow water as illustrated in Figure 2. Mass gain was recorded from 1 min to 7 days, and cumulative absorption computed as:

$$I(t) = \left(\frac{M_t - M_0}{A\rho_w} \right)$$

where m is in g, A is the exposed-face area (7,854 mm² for 100-mm diameter), $\rho_w = 0.001$ g/mm³, and I in mm. Initial (1–6 h) and secondary (1–7 d) sorptivity were obtained by least-squares regression of I (mm) versus $(t)^{1/2}$, in mm s^{-1/2}; if the full-interval fit did not achieve $r \geq 0.98$, the value was designated as Not Determined (ND).



Fig. 2. Sorptivity Setup: oven-drying; sealed conditioning; and sealing of all faces except the exposed face (shallow water contact).

III. RESULTS AND DISCUSSIONS

A. Compressive Strength

Figures 3 and 4 illustrate the compressive strength of geopolymer mortar at 14 and 28 days for mixes with different SP dosages (SP0–SP3) and alkaline solution ratios (R1–R2.5). At 28 days, strength increased steadily with higher alkaline ratios. For example, SP0 increased from 4.25 MPa at R1 to 7.70 MPa at R2.5, while SP3 improved from 6.75 to 12.61 MPa. Adding SP increased the compressive strength by about 60%, showing its role in supporting long-term strength. At 14 days, the influence of SP was most obvious at the lower alkaline ratio: at R1, SP3 more than doubled the strength compared with SP0. At R2.5, the increase was smaller but still noticeable. Overall, the alkaline ratio was the main driver of strength gain, while SP helped by improving compaction and reducing voids. As the alkaline solution ratio increases, the molar ratio of SiO₂/Na₂O in the solution also increases, with values of 1.06, 1.38, 1.62, and 1.80 corresponding to alkaline solution ratios of 1, 1.5, 2, and 2.5, respectively. Mechanical and morphological properties of geopolymer are influenced by the molar ratio of SiO₂ to Na₂O [34–36]. Higher ratios promoted denser matrices, consistent with the trend reported by authors in [36].

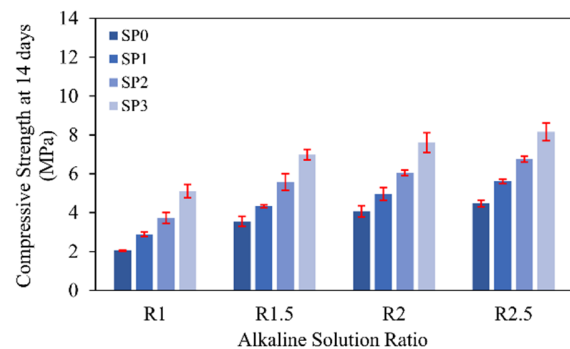


Fig. 3. Compressive strength of geopolymer mortar at 14 days.

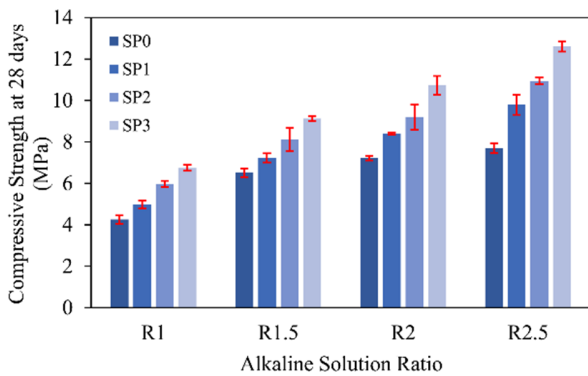


Fig. 4. Compressive strength of geopolymer mortar at 28 days.

Figure 5 shows the effect of curing methods. Specimens wrapped in damp cloth reached strengths 5–17% higher than those kept at room temperature. This suggests moist curing is a practical option in the field. Heat curing can accelerate geopolymerization, but it is energy-demanding and less realistic for in-situ work [37-42]. These results confirm that ambient or moist curing can deliver sufficient strength for structural use without relying on high-temperature treatment.

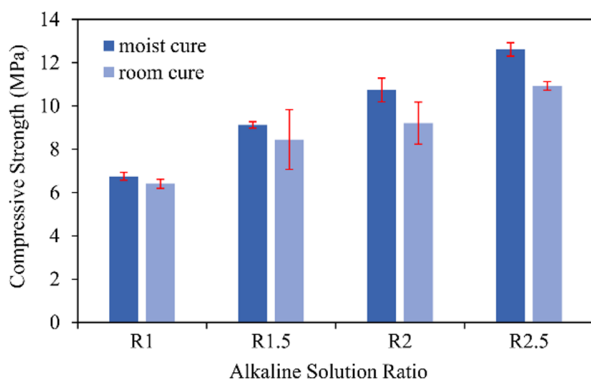


Fig. 5. Effect of curing on compressive strength of geopolymer mortar.

B. Water Absorption, Density, and Porosity

Table II presents the physical properties of the geopolymer mortar after 28 days, while Figure 6 illustrates their relationship with compressive strength. Water absorption dropped from 6.59±0.09% at R1 to 5.47±0.18% at R2.5, while porosity declined from 21.15±3.11% to 11.56±6.97%. At the same time, bulk density increased from 1.66±0.11 Mg/m³ to 2.31±0.25 Mg/m³, pointing to a denser internal structure. These changes were closely tied to strength. Mixtures with higher density and lower porosity consistently carried greater loads, whereas higher absorption and porosity weakened the matrix ($R^2 > 0.67$). Similar links between pore structure and strength have been reported before, with absorption reflecting pore connectivity [43], and denser mixes showing better performance [44, 45]. On the micro level, increasing the Na₂SiO₃/NaOH ratio enhances aluminosilicate dissolution and gel production, forming N–A–S–H and C–(A)–S–H phases that fill voids, reduce porosity, and strengthen bonding [46].

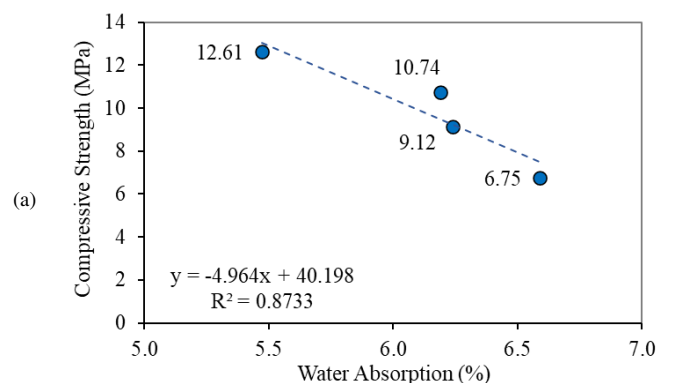
CM showed a water absorption of 7.26±0.33%, an apparent density of 2.16 Mg/m³, and a porosity of 10.18±0.65%. Compared with geopolymer mortar, it had slightly lower porosity but absorbed more water. Authors in [43] observed similar results in mortars made with metakaolin and GGBFS. Overall, the data confirm that pore structure strongly governs performance: mortars with fewer voids not only absorbed less water but also developed higher strength.

TABLE II. PHYSICAL PROPERTIES OF GEOPOLYMER MORTAR-SP3 MIXES

Parameter	Mix ID				
	SP3-R1	SP3-R1.5	SP3-R2	SP3-R2.5	CM
Water absorption (%)	6.59±0.09	6.24±0.15	6.19±0.22	5.47±0.18	7.26±0.33
Bulk density, dry (Mg/m ³)	1.66±0.11	1.69±0.05	1.79±0.09	2.31±0.25	1.94±0.03
Apparent density (Mg/m ³)	2.11±0.14	2.15±0.28	2.23±0.20	2.60±0.07	2.16±0.02
Volume of permeable voids (%)	21.15±3.11	20.83±6.12	19.84±3.42	11.56±6.97	10.18±0.65

C. Sorptivity

The combined results from Figure 7 and Table II highlight a clear difference between geopolymer mortars and CM in terms of sorptivity, porosity, and water absorption. All mixes show the expected two-phase $I-\sqrt{t}$ response. The CM exhibits the steepest initial slope ($S_i=0.049 \text{ mm s}^{-1/2}$) and the lowest secondary slope ($S_s=0.00071 \text{ mm s}^{-1/2}$). For the geopolymers, the 1–6 h segment did not consistently meet the ASTM linearity criterion ($r \geq 0.98$); therefore, S_i is reported as ND, and the early-time rise is discussed qualitatively (lowest for R1–R1.5, intermediate for R2.5, highest for R2). In contrast, secondary sorptivity is reportable for all geopolymers (0.0008–0.0023 $\text{mm s}^{-1/2}$, minimum at R1.5). Water absorption ranks differently: CM = 7.26% exceeds the geopolymers (5.47–6.59%), with SP3-R2.5 the lowest (5.47%). This indicates that rate (sorptivity) and capacity (absorption/voids) are decoupled: near-surface connectivity governs early ingress, whereas a finer/tortuous network controls the later stage and cumulative uptake. Accordingly, SP3-R2.5 can achieve the highest strength and lowest absorption yet still not minimize the early-time rate—consistent with prior reports [43, 47-50].



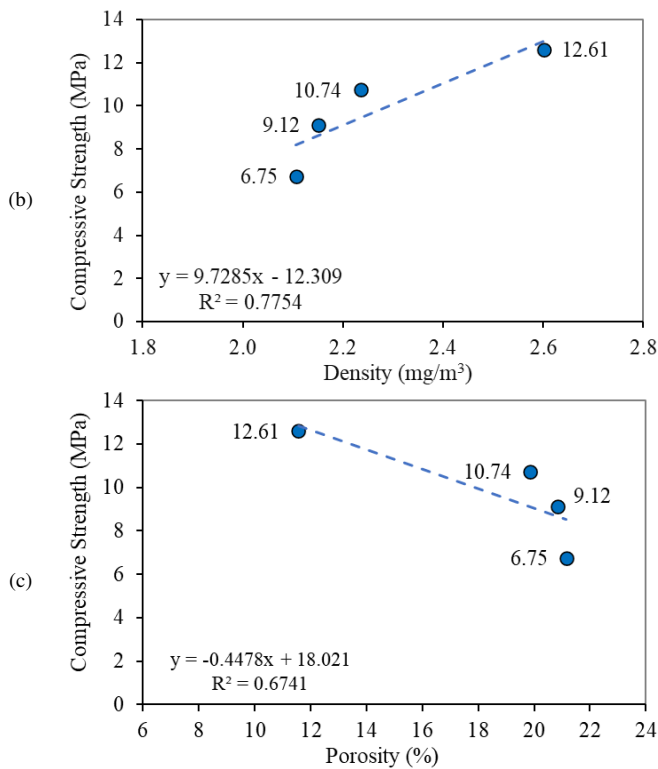


Fig. 6. Physical properties affecting compressive strength: (a) water absorption; (b) density; (c) porosity.

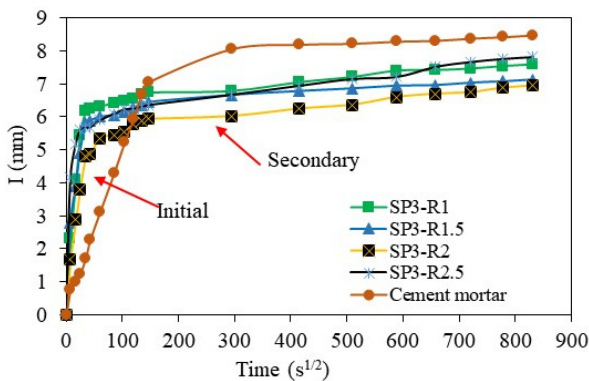


Fig. 7. Cumulative absorption, I (mm), versus $\sqrt{\text{time } (t)} (s^{1/2})$.

D. Durability of Geopolymer Mortar

Durability was evaluated on geopolymer mortar with an alkaline ratio of 2.5 and 0.3% SP, compared with CM. After 28 days of curing, specimens were exposed to sulfuric acid (pH 3) for up to three months. Two conditions were applied: full immersion (F) and wet-dry cycles (WD). Acidic water (A) represented the aggressive environment, while neutral water (N) served as the control. Compressive strength was measured after 1, 2, and 3 months, as shown in Figures 8 and 9.

As shown in Figure 8, FA geopolymer mortar performed remarkably well in acid. In immersion, its compressive strength increased by 17.2% after one month and by 21.5% at the end of three months. This trend indicates that unreacted FA continued to dissolve and contribute to the formation of N-A-S-H gels,

which refined the pore structure and improved matrix density. Under wet-dry cycles, the pattern was different: strength first increased (10.9% at one month) but then declined slightly, reaching a loss of 5.3% at three months. The reduction is attributed to microcracks generated during drying, which acted as pathways for acid ingress. Authors in [51] described the same mechanism in cyclic preloading tests, where cracks accelerated the deterioration of geopolymers in acid environments.

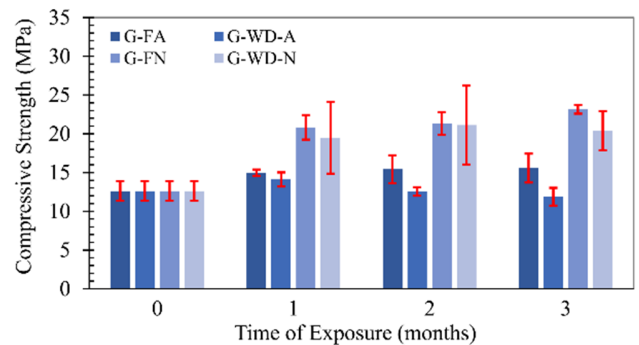


Fig. 8. Effect of tidal acidic exposure on the compressive strength of geopolymer mortar.

Cement mortar, by contrast, followed the classic path of deterioration, as shown in Figure 9. Its strength fell nearly 50% after three months of acid immersion and almost 30% under wet-dry cycles. The difference stems from binder chemistry: calcium hydrates (C-S-H, $Ca(OH)_2$) are unstable in acid, forming gypsum and ettringite that expand, crack the matrix, and accelerate attack. Authors in [52, 53] emphasized that calcium hydrates are the weak link in OPC, while low-calcium geopolymers based on N-A-S-H are far more stable. The role of calcium was consistent with the findings in [29], where small cement additions gave short-term strength gains after acid exposure due to pore filling by ettringite. Authors in [54] described the same two-stage effect: early densification, followed by expansion and cracking once ettringite exceeded pore capacity. Reviews of slag-FA blends confirm this trade-off—higher calcium contents improve early strength but compromise long-term durability [55].

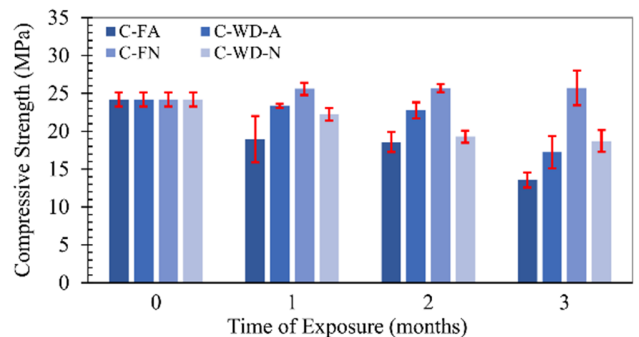


Fig. 9. Effect of tidal acidic exposure on the compressive strength of cement mortar.

The neutral water results provide further insight. In full immersion, the geopolymer mortar continued to gain strength steadily, reaching a 76.4% increase after three months. This indicates that geopolymerization was still progressing beyond 28 days, with unreacted FA gradually incorporated into the N–A–S–H network. Cement mortar, in contrast, gained only about 6% in full immersion. This suggests that calcium leaching weakens the cement matrix even in non-aggressive water. The neutral water controls reinforced these findings. Geopolymer mortar continued to gain strength, reaching a 76.4% increase under immersion and maintaining more than 50% improvement under wet-dry cycles after three months. Cement mortar, however, first showed minor gains (~6%) before losing 22–23% of its strength, whether immersed or cycled. This behavior reflects ongoing geopolymerization in FA systems, while calcium leaching and microcracking dominate OPC. These results align with reviews that highlight the superior chemical stability of N–A–S–H gels compared with calcium hydrates, as well as the role of microstructure in long-term durability [56, 57].

In summary, the results clearly demonstrate that FA geopolymers outperformed cement mortar under both acidic and neutral exposures. Strength gains in immersion, limited losses under acid cycles, and consistent improvement in neutral water confirm the durability of low-Ca geopolymers. By contrast, cement mortars suffered severe degradation in acid and progressive leaching in neutral water, underscoring their vulnerability. Unlike many earlier studies focused only on acid-induced strength loss, this work links porosity, absorption, and sorptivity with durability under tidal cycles, providing a more complete view of long-term performance. Moreover, by using FA from the Asam-Asam Power Plant, the study shows how local industrial byproducts can be transformed into durable and sustainable binders for coastal environments.

IV. CONCLUSION

This study examined geopolymer mortar made with Fly Ash (FA) from the Asam-Asam Power Plant, focusing on strength, pore structure, water transport, and durability in tidal acidic exposure. Strength improved with higher alkaline ratios, and the addition of 0.3% superplasticizer (SP) gave the best results. Denser mixes with lower porosity and absorption also reached higher strength, confirming that pore structure plays a central role. Sorptivity confirmed the expected two-phase capillary behavior. While secondary sorptivity was lowest for R1.5, the lowest water absorption occurred at R2.5, indicating a partial decoupling between early-time rate and cumulative uptake. When exposed to sulfuric acid, the difference between binders was clear. Geopolymer mortar gained strength in immersion and showed only small losses in wet-dry cycles, while cement mortar deteriorated rapidly. Its aluminosilicate gel network provided stability at low pH, unlike cement hydrates that reacted to form gypsum and ettringite. In short, the study shows that pore structure and transport properties significantly control long-term performance. Using local FA, geopolymer mortar proved to be a durable and sustainable material for tidal acidic exposure.

ACKNOWLEDGMENT

The authors would like to thank the Ministry of Research, Technology, and Higher Education of the Republic of Indonesia for their financial support through the DRTPM (BIMA) Research Grant Program under contract number 056/E5/PG.02.00.PL/2024 and derivative contract number 1006/UN8.2/PG/2024. The authors also extend their gratitude to the Structures and Materials Laboratory of the Civil Engineering Faculty, Lambung Mangkurat University.

REFERENCES

- [1] H. G. Van Oss and A. C. Padovani, "Cement Manufacture and the Environment: Part I: Chemistry and Technology," *Journal of Industrial Ecology*, vol. 6, no. 1, pp. 89–105, Jan. 2002, <https://doi.org/10.1162/108819802320971650>.
- [2] A. Bosoaga, O. Masek, and J. E. Oakey, "CO₂ Capture Technologies for Cement Industry," *Energy Procedia*, vol. 1, no. 1, pp. 133–140, Feb. 2009, <https://doi.org/10.1016/j.egypro.2009.01.020>.
- [3] P. V. Nidheesh and M. S. Kumar, "An overview of Environmental Sustainability in Cement and Steel Production," *Journal of Cleaner Production*, vol. 231, pp. 856–871, Sept. 2019, <https://doi.org/10.1016/j.jclepro.2019.05.251>.
- [4] A. Pal, "Developing Low-Clinker Ternary Blends for Indian Cement Industry," *Journal of The Institution of Engineers (India): Series A*, vol. 99, no. 3, pp. 433–447, Sept. 2018, <https://doi.org/10.1007/s40030-018-0309-4>.
- [5] W. Shanks, C. F. Dunant, M. P. Drewniok, R. C. Lupton, A. Serrenho, and J. M. Allwood, "How Much Cement Can We Do Without? Lessons From Cement Material Flows in the UK," *Resources, Conservation and Recycling*, vol. 141, pp. 441–454, Feb. 2019, <https://doi.org/10.1016/j.resconrec.2018.11.002>.
- [6] Z. He, X. Zhu, J. Wang, M. Mu, and Y. Wang, "Comparison of CO₂ Emissions from OPC and Recycled Cement Production," *Construction and Building Materials*, vol. 211, pp. 965–973, June 2019, <https://doi.org/10.1016/j.conbuildmat.2019.03.289>.
- [7] T. W. S. Panjaitan, P. Dargusch, D. Wadley, and A. A. Aziz, "Meeting International Standards of Cleaner Production in Developing Countries: Challenges and Financial Realities Facing the Indonesian Cement Industry," *Journal of Cleaner Production*, vol. 318, Oct. 2021, Art. no. 128604, <https://doi.org/10.1016/j.jclepro.2021.128604>.
- [8] W. Lan and C. Yuansheng, "The Application and development of Fly Ash in China," *2007 World of Coal Ash*, Covington, KY, USA, May 2007.
- [9] C.-H. Huang, S.-K. Lin, C.-S. Chang, and H.-J. Chen, "Mix Proportions and Mechanical Properties of Concrete Containing Very High-Volume of Class F Fly Ash," *Construction and Building Materials*, vol. 46, pp. 71–78, Sept. 2013, <https://doi.org/10.1016/j.conbuildmat.2013.04.016>.
- [10] P. Van Den Heede, C. Thiel, and N. De Belie, "Natural and Accelerated Carbonation Behaviour of High-Volume Fly Ash (HVFA) Mortar: Effects on Internal Moisture, Microstructure and Carbonated Phase Proportioning," *Cement and Concrete Composites*, vol. 113, Oct. 2020, Art. no. 103713, <https://doi.org/10.1016/j.cemconcomp.2020.103713>.
- [11] G. S. Ryu, Y. B. Lee, K. T. Koh, and Y. S. Chung, "The Mechanical Properties of Fly Ash-based Geopolymer Concrete with Alkaline Activators," *Construction and Building Materials*, vol. 47, pp. 409–418, Oct. 2013, <https://doi.org/10.1016/j.conbuildmat.2013.05.069>.
- [12] A. M. Fernández-Jiménez, A. Palomo, and C. López-Hombrados, "Engineering Properties of Alkali-Activated Fly Ash Concrete," *ACI Materials Journal*, vol. 103, no. 2, pp. 106–4112, 2006, <https://doi.org/10.14359/15261>.
- [13] D. Hardjito, C. C. Cheak, and C. H. Lee Ing, "Strength and Setting Times of Low Calcium Fly Ash-based Geopolymer Mortar," *Modern Applied Science*, vol. 2, no. 4, pp. 3–11, July 2008, <https://doi.org/10.5539/mas.v2n4p3>.
- [14] P. Nath and P. K. Sarker, "Use of OPC to Improve Setting and Early Strength Properties of Low Calcium Fly Ash Geopolymer Concrete

- Cured at Room Temperature," *Cement and Concrete Composites*, vol. 55, pp. 205–214, Jan. 2015, <https://doi.org/10.1016/j.cemconcomp.2014.08.008>.
- [15] A. R. Saïdy, B. J. Priatmadi, and M. Septiana, "Reduction in Carbon Dioxide and Methane Production of Tropical Peatlands Due to Coal Fly-Ash Application," *IOP Conference Series: Earth and Environmental Science*, vol. 976, no. 1, Feb. 2022, Art. no. 012022, <https://doi.org/10.1088/1755-1315/976/1/012022>.
- [16] I. Prasetya, M. Syaui, and A. S. Aini, "Application of central Kalimantan Coal ash as a Sustainable Construction Material," *IOP Conference Series: Earth and Environmental Science*, vol. 758, no. 1, Apr. 2021, Art. no. 012011, <https://doi.org/10.1088/1755-1315/758/1/012011>.
- [17] I. Prasetya and M. F. Rizani, "Analysis of Fly Ash from PLTU Asam-Asam as a Construction Material in Terms of its Physical and Mechanical Properties," *MATEC Web of Conferences*, vol. 280, 2019, Art. no. 04013, <https://doi.org/10.1051/mateconf/201928004013>.
- [18] R. Nurwidayati, M. B. Ulum, J. J. Ekaputri, Triwulan, and P. Suprobo, "Characterization of Fly Ash on Geopolymer Paste," *Materials Science Forum*, vol. 841, pp. 118–125, Jan. 2016, <https://doi.org/10.4028/www.scientific.net/MSF.841.118>.
- [19] L. N. Assi, E. (Eddie) Deaver, M. K. ElBatanouny, and P. Ziehl, "Investigation of Early Compressive Strength of Fly Ash-based Geopolymer Concrete," *Construction and Building Materials*, vol. 112, pp. 807–815, June 2016, <https://doi.org/10.1016/j.conbuildmat.2016.03.008>.
- [20] T. Bualuang, P. Jitsangiam, N. Chusai, T. Suwan, U. Rattanasak, and P. Chindaprasirt, "Utilization of Dumped Coal Ash from Power-Plant Landfills for Carbon Footprint Reduction in Sustainable Pavement Base Construction," *Construction and Building Materials*, vol. 441, Aug. 2024, Art. no. 137462, <https://doi.org/10.1016/j.conbuildmat.2024.137462>.
- [21] N. H. Haryanti, N. Chairunnisa, A. Y. Pratiwi, R. Nurwidayati, and W. A. Krasna, "Physical and Mechanical Properties of Geopolymers with the Addition of NaOH Modified Bemban Fiber (Donax Canniformis)," *Engineering, Technology & Applied Science Research*, vol. 15, no. 2, pp. 21144–21151, Apr. 2025, <https://doi.org/10.48084/etasr.9953>.
- [22] M. A. M. Ariffin, M. A. R. Bhutta, M. W. Hussin, M. Mohd Tahir, and N. Aziah, "Sulfuric acid Resistance of Blended Ash Geopolymer Concrete," *Construction and Building Materials*, vol. 43, pp. 80–86, June 2013, <https://doi.org/10.1016/j.conbuildmat.2013.01.018>.
- [23] I. T. Wicaksono and R. Nurwidayati, "The Effect of pH Water on the Concrete Mixtures and Curing Condition on the Compressive Strength of Concrete," *IOP Conference Series: Earth and Environmental Science*, vol. 999, no. 1, Mar. 2022, Art. no. 012006, <https://doi.org/10.1088/1755-1315/999/1/012006>.
- [24] V. Zivica and A. Bajza, "Acidic Attack of Cement Based Materials — a Review," *Construction and Building Materials*, vol. 15, no. 8, pp. 331–340, Dec. 2001, [https://doi.org/10.1016/S0950-0618\(01\)00012-5](https://doi.org/10.1016/S0950-0618(01)00012-5).
- [25] F. N. Okoye, S. Prakash, and N. B. Singh, "Durability of Fly Ash Based Geopolymer Concrete in the Presence of Silica Fume," *Journal of Cleaner Production*, vol. 149, pp. 1062–1067, Apr. 2017, <https://doi.org/10.1016/j.jclepro.2017.02.176>.
- [26] V. Sata, A. Sathonsaowaphak, and P. Chindaprasirt, "Resistance of Lignite Bottom Ash Geopolymer Mortar to Sulfate and Sulfuric Acid Attack," *Cement and Concrete Composites*, vol. 34, no. 5, pp. 700–708, May 2012, <https://doi.org/10.1016/j.cemconcomp.2012.01.010>.
- [27] T. Suresh, G. Partha, and G. Somnath, "Resistance of Fly Ash Based Geopolymer Mortars in Sulfuric Acid," *ARP Journal of Engineering and Applied Sciences*, vol. 4, no. 1, pp. 65–70, Feb. 2009.
- [28] R. Yanuari, D. Septari, J. A. Rindy, and M. Olivia, "Geopolymer Hybrid Fly Ash Concrete for Construction and Conservation in Peat Environment: A Review," *IOP Conference Series: Earth and Environmental Science*, vol. 847, no. 1, Sept. 2021, Art. no. 012031, <https://doi.org/10.1088/1755-1315/847/1/012031>.
- [29] R. Nurwidayati, H. Haryanti, N. Chairunnisa, A. Y. Pratiwi, W. A. Krasna, and N. Rahmadania, "Investigating the Impact of Fly Ash Replacement with Portland Cement on Porosity, Water Absorption, and Compressive Strength of Geopolymer Mortars in a Tidal Acid Environment," *Engineering, Technology & Applied Science Research*, vol. 15, no. 6, pp. 21144–21151, 2025, <https://doi.org/10.48084/etasr.13667>.
- [30] *Standard Specification for Coal Fly Ash and Raw or Calcined Natural Pozzolan for Use in Concrete*, ASTM C618-22, ASTM International, West Conshohocken, PA, USA, 2022.
- [31] *Standard Test Method for Compressive Strength of Hydraulic Cement Mortars (Using 2-in. or [50-mm] Cube Specimens)*, ASTM C109/C109M-20, ASTM International, West Conshohocken, PA, USA, 2020.
- [32] *Standard Test Method for Density, Absorption, and Voids in Hardened Concrete*, ASTM C642-21, ASTM International, West Conshohocken, PA, USA, 2021.
- [33] *Standard Test Method for Measurement of Rate of Absorption of Water by Hydraulic-Cement Concretes*, ASTM C642-21, ASTM International, West Conshohocken, PA, USA, 2020.
- [34] J. Cai, J. Pan, J. Han, and X. Wang, "Mechanical Behaviors of Metakaolin-Based Engineered Geopolymer Composite under Ambient Curing Condition," *Journal of Materials in Civil Engineering*, vol. 34, no. 7, July 2022, Art. no. 04022152, [https://doi.org/10.1061/\(ASCE\)MT.1943-5533.0004304](https://doi.org/10.1061/(ASCE)MT.1943-5533.0004304).
- [35] A. S. De Vargas, D. C. C. Dal Molin, A. C. F. Vilela, F. J. D. Silva, B. Pavão, and H. Veit, "The Effects of Na₂O/SiO₂ Molar Ratio, Curing Temperature and Age on Compressive Strength, Morphology and Microstructure of Alkali-Activated Fly Ash-Based Geopolymers," *Cement and Concrete Composites*, vol. 33, no. 6, pp. 653–660, July 2011, <https://doi.org/10.1016/j.cemconcomp.2011.03.006>.
- [36] K. Gao *et al.*, "Effects of SiO₂/Na₂O Molar Ratio on Mechanical Properties and the Microstructure of Nano-SiO₂ Metakaolin-Based Geopolymers," *Construction and Building Materials*, vol. 53, pp. 503–510, Feb. 2014, <https://doi.org/10.1016/j.conbuildmat.2013.12.003>.
- [37] C. D. Atiş, E. B. Görür, O. Karahan, C. Bilim, S. İlkentapar, and E. Luga, "Very High Strength (120 Mpa) Class F Fly Ash Geopolymer Mortar Activated at Different NaOH Amount, Heat Curing Temperature and Heat Curing Duration," *Construction and Building Materials*, vol. 96, pp. 673–678, Oct. 2015, <https://doi.org/10.1016/j.conbuildmat.2015.08.089>.
- [38] P. Topark-Ngarm, P. Chindaprasirt, and V. Sata, "Setting Time, Strength, and Bond of High-Calcium Fly Ash Geopolymer Concrete," *Journal of Materials in Civil Engineering*, vol. 27, no. 7, July 2015, Art. no. 04014198, [https://doi.org/10.1061/\(ASCE\)MT.1943-5533.0001157](https://doi.org/10.1061/(ASCE)MT.1943-5533.0001157).
- [39] M. Z. N. Khan, F. U. A. Shaikh, Y. Hao, and H. Hao, "Synthesis of High Strength Ambient Cured Geopolymer Composite by Using Low Calcium Fly Ash," *Construction and Building Materials*, vol. 125, pp. 809–820, Oct. 2016, <https://doi.org/10.1016/j.conbuildmat.2016.08.097>.
- [40] P. Nath, P. K. Sarker, and V. B. Rangan, "Early Age Properties of Low-Calcium Fly Ash Geopolymer Concrete Suitable for Ambient Curing," *Procedia Engineering*, vol. 125, pp. 601–607, 2015, <https://doi.org/10.1016/j.proeng.2015.11.077>.
- [41] P. Wattanachai and T. Suwan, "Strength of Geopolymer Cement Curing at Ambient Temperature by Non-Oven Curing Approaches: An Overview," *IOP Conference Series: Materials Science and Engineering*, vol. 212, June 2017, Art. no. 012014, <https://doi.org/10.1088/1757-899X/212/1/012014>.
- [42] B. Nematollahi, J. Sanjayan, and F. U. A. Shaikh, "Synthesis of Heat and Ambient Cured One-part Geopolymer Mixes With Different Grades of Sodium Silicate," *Ceramics International*, vol. 41, no. 4, pp. 5696–5704, May 2015, <https://doi.org/10.1016/j.ceramint.2014.12.154>.
- [43] M. Ka, D. Hoffmann, L. Molez, and C. Lanos, "Alkali-activated Mortars: Porosity and Capillary Absorption," *European Journal of Environmental and Civil Engineering*, vol. 27, no. 4, pp. 1715–1729, Mar. 2023, <https://doi.org/10.1080/19648189.2022.2094467>.
- [44] S. Thokchom, P. Ghosh, and S. Ghosh, "Effect of Water Absorption, Porosity and Sorptivity on Durability of Geopolymer Mortars," *ARP Journal of Engineering and Applied Sciences*, vol. 4, no. 7, pp. 28–32, Sept. 2009.
- [45] I. Balczár, T. Korim, and A. Dobrádi, "Correlation of Strength to Apparent Porosity of Geopolymers – Understanding Through Variations

- of Setting Time," *Construction and Building Materials*, vol. 93, pp. 983–988, Sept. 2015, <https://doi.org/10.1016/j.conbuildmat.2015.05.059>.
- [46] M. H. Raza, M. Khan, and R. Y. Zhong, "Strength, Porosity and Life Cycle Analysis of Geopolymer and Hybrid Cement Mortars for Sustainable Construction," *Science of The Total Environment*, vol. 907, Jan. 2024, Art. no. 167839, <https://doi.org/10.1016/j.scitotenv.2023.167839>.
- [47] B. Aïssoun, K. Khayat, and J.-L. Gallias, "Variations of Sorptivity with Rheological Properties of Concrete Cover in Self-consolidating Concrete," *Construction and Building Materials*, vol. 113, pp. 113–120, June 2016, <https://doi.org/10.1016/j.conbuildmat.2016.03.006>.
- [48] M. Albitar, M. S. Mohamed Ali, P. Visintin, and M. Drechsler, "Durability Evaluation of Geopolymer and Conventional Concretes," *Construction and Building Materials*, vol. 136, pp. 374–385, Apr. 2017, <https://doi.org/10.1016/j.conbuildmat.2017.01.056>.
- [49] C. Chotetanorn, P. Chindaprasirt, V. Sata, S. Rukzon, and A. Sathonsaowaphak, "High-Calcium Bottom Ash Geopolymer: Sorptivity, Pore Size, and Resistance to Sodium Sulfate Attack," *Journal of Materials in Civil Engineering*, vol. 25, no. 1, pp. 105–111, Jan. 2013, [https://doi.org/10.1061/\(ASCE\)MT.1943-5533.0000560](https://doi.org/10.1061/(ASCE)MT.1943-5533.0000560).
- [50] W. Kubissa and R. Jaskulski, "Measuring and Time Variability of the Sorptivity of Concrete," *Procedia Engineering*, vol. 57, pp. 634–641, 2013, <https://doi.org/10.1016/j.proeng.2013.04.080>.
- [51] F. Qu, W. Li, K. Wang, S. Zhang, and D. Sheng, "Performance Deterioration of Fly Ash/slag-based Geopolymer Composites Subjected to Coupled Cyclic Preloading and Sulfuric Acid Attack," *Journal of Cleaner Production*, vol. 321, Oct. 2021, Art. no. 128942, <https://doi.org/10.1016/j.jclepro.2021.128942>.
- [52] H. S. Abhishek, S. Prashant, M. V. Kamath, and M. Kumar, "Fresh Mechanical and Durability Properties of Alkali-activated Fly Ash-slag Concrete: A Review," *Innovative Infrastructure Solutions*, vol. 7, no. 1, Feb. 2022, Art. no. 116, <https://doi.org/10.1007/s41062-021-00711-w>.
- [53] S. Magotra and A. A. Jee, "A Review on Durability and Microstructure of Fly-ash Based Geopolymer Concrete (FA-GPC)," *Materials Today: Proceedings*, June 2024, Art. no. S2214785324004668, <https://doi.org/10.1016/j.matpr.2024.06.011>.
- [54] F. Xie, J. Li, G. Zhao, C. Wang, Y. Wang, and P. Zhou, "Experimental Investigations on the Durability and Degradation Mechanism of Cast-in-situ Recycled Aggregate Concrete Under Chemical Sulfate Attack," *Construction and Building Materials*, vol. 297, Aug. 2021, Art. no. 123771, <https://doi.org/10.1016/j.conbuildmat.2021.123771>.
- [55] S. Aldawsari, R. Kampmann, J. Harnisch, and C. Rohde, "Setting Time, Microstructure, and Durability Properties of Low Calcium Fly Ash/Slag Geopolymer: A Review," *Materials*, vol. 15, no. 3, Jan. 2022, Art. no. 876, <https://doi.org/10.3390/ma15030876>.
- [56] J. S. J. Van Deventer, J. L. Provis, and P. Duxson, "Technical and Commercial Progress in the Adoption of Geopolymer Cement," *Minerals Engineering*, vol. 29, pp. 89–104, Mar. 2012, <https://doi.org/10.1016/j.mineng.2011.09.009>.
- [57] M. N. S. Hadi, M. Al-Azzawi, and T. Yu, "Effects of Fly Ash Characteristics and Alkaline Activator Components on Compressive Strength of Fly Ash-based Geopolymer Mortar," *Construction and Building Materials*, vol. 175, pp. 41–54, June 2018, <https://doi.org/10.1016/j.conbuildmat.2018.04.092>.